Characterization of porous acoustic materials

Walter Lauriks, Laurens Boeckx, Philippe Leclaire

▶ **To cite this version:**

Walter Lauriks, Laurens Boeckx, Philippe Leclaire. Characterization of porous acoustic materials. SAPEM 2005 Symposium on the Acoustics of Poro-Elastic Materials, Dec 2005, Lyon, France. hal-01329870

HAL Id: hal-01329870
https://hal.science/hal-01329870

Submitted on 9 Jun 2016

HAL is a multi-disciplinary open access archive for the deposit and dissemination of scientific research documents, whether they are published or not. The documents may come from teaching and research institutions in France or abroad, or from public or private research centers.

L'archive ouverte pluridisciplinaire **HAL**, est destinée au dépôt et à la diffusion de documents scientifiques de niveau recherche, publiés ou non, émanant des établissements d'enseignement et de recherche français ou étrangers, des laboratoires publics ou privés.

Distributed under a Creative Commons Attribution 4.0 International License

Characterization of porous acoustic materials

W. Lauriks, L. Boeckx and P. Leclaire

Laboratorium voor Akoestiek en Thermische Fysica, Departement Natuurkunde
Celestijnenlaan 200D, 3001 Heverlee, België

An overview of the models and parameters of the acoustic wave propagation in porous media is presented. The most common parameters (the porosity, the permeability or flow resistivity and the densities) can be measured with standard methods. Ultrasonic methods for measuring the other parameters (the tortuosity and characteristic lengths) related to the complex pore micro-structure are reviewed. The ultrasonic methods are based on the transmission or reflection of airborne ultrasonic waves and on the signal analysis in the frequency and/or in the time domains. Ultrasonic scattering is discussed at higher frequencies where the classical models are no longer valid. In order to complete the characterization of porous acoustic materials, new techniques for evaluating the elastic and viscoelastic properties are proposed. These techniques are based on the generation of standing waves in a layer of material and on the spatial Fourier Transform of the displacement profile of the upper surface. Two configurations are proposed: a layer of porous material glued on a rigid substrate and a porous layer under Lamb conditions. Theoretical dispersion curves are fitted to the experimental results and this procedure can provide information on the complex shear modulus and of the complex Poisson ratio in a wide frequency range, typically between 50 Hz and 4 kHz.

1 Introduction

Porous media are of great interest in geophysics, in the petroleum research, in the automobile and building industries or in medical sciences with ultrasonic propagation in bones. The interest for the wave propagation in porous media started with Lord Rayleigh at the end of the XIX^{th} century. Later, in the nineteen fourties, Zwikker and Kosten [1] proposed a model of the wave propagation in porous materials with cylindrical pores including viscous and thermal interactions between the solid and the fluid. In 1956, M. A. Biot [2] published an elaborate model of the elastic wave propagation in fluid saturated porous media including the different coupling mechanisms between the phases, the wave attenuation due to the viscous frictions and the elasticity of the solid skeleton. Yet, Biot's theory remained relatively ignored until the years 70-80. The scientific community realized in these years the great potential of this theory. The interest for porous media has not ceased since then and many acoustic models developed recently are derived from Biot's theory.

Figure 1 shows an example of porous material, a highly porous reticulated (with open pores) polyurethane foam often used in acoustic engineering. The porosity in such materials can be greater than 95 % (the porosity is defined further down in this study). The choice of this example of material does not restricts the generality of the following results.

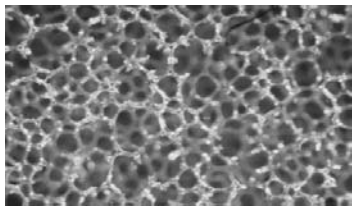

Figure 1: Example of porous material: a highly porous reticulated polyurethane foam.

This type of material can be seen as a collection of solid bonds linked together and forming 3-D structures such as dodecahedras. It is difficult for these materials to speak of "pores". However, lacking of more appropriate terminology, we shall use this term for the rest of this study, the pore being "the space not occupied by the solid".

The theoretical description of wave propagation in such materials has constantly progressed, particularly since the years 70-80 with the contribution of many researcher. Along with the theoretical developments, experimental techniques were invented for the measurement of the relevant basic physical parameters of porous media. The measurement of porosity [4, 5], phase densities and flow resistivity [6] are now standard. However, the main disadvantage of the most elaborate models was the necessity to determine certain other parameters acting at high frequencies and closely related to the pore structure at the pore scale.

In this article, an overview of the models and parameters of the acoustic wave propagation in porous media is given. Techniques developed in K. U. Leuven and in Le Mans for determining high frequency physical parameters and also the elastic properties of porous materials are then presented. The use of these technique have resulted in the characterization of acoustic materials without adjustable parameters for the first time and to the description of wave propagation at high frequencies where models based on effective phases (among which is Biot's theory) are no longer valid and must make way to diffusion models. The frequency domains are defined in Figure 2.

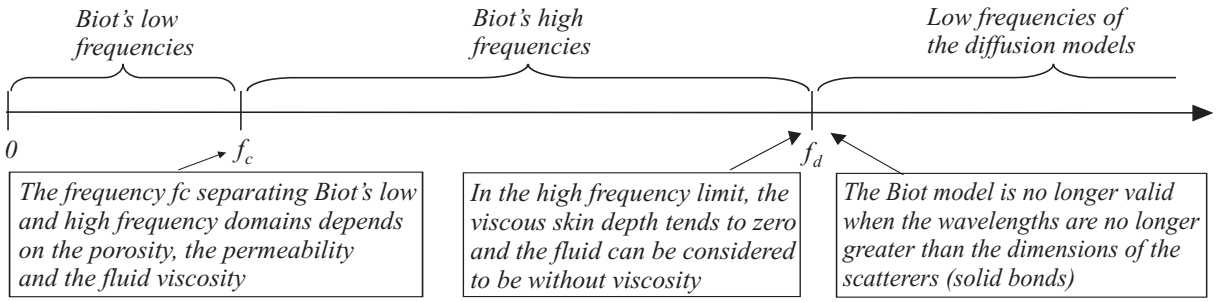

Figure 2: Frequency domains in the Biot model.

2 Models and parameters of the acoustic wave propagation in porous media

2.1 Biot's theory

The main qualitative results of Biot's theory are briefly recalled in this sections. For more details, the reader is referred to the original article by Biot [2] or to the book by Allard [3] for example. The elastic wave propagation in fluid-saturated porous media is considered for wavelengths greater than the characteristic dimensions of the heterogeneities. When the fluid and the solid have compressibilities and densities of the same order of magnitude, energy exchanges of two types can occur in a lossless propagation: the exchange of momentum and the elastic couplings.

The elastic couplings are expressed in Biot's coupled equation of poroelasticity and the momentum exchanges in Biot's coupled equations of motion. In his first formulation, the solid and the fluid are treated on equal foot as effective phases standing for the real phases. The problem is treated as an eigenvalue problem with the existence of several modes that are solutions of the coupled equations of motion. Two compressional and one shear waves are predicted in the general case when both the solid and the fluid the phases are connected and percolating. The consequence of coupling in a mechanical system is the repulsion of the eigenvalues when they get closer and attempt to cross each other. The eigenvalues of the coupled system (the velocities) cannot cross and a fast and a slow waves are predicted. These were called respectively waves of the first kind and of the second kind.

The phase velocity of each mode is obtained from the eigenvalues of $\tilde{R}^{-1}\tilde{\rho}$ where $\tilde{R}$ is a rigidity matrix and $\tilde{\rho}$ is a density matrix. The crossed terms in these matrices are the coefficients of the elastic coupling and momentum exchange terms. The coefficients of these matrices are given in Refs [2, 7] and depend on the material properties: the porosity, the solid and fluid densities and also the elastic moduli of the solid, of the fluid and of the solid frame.

Wave attenuation by viscous friction are included in the model through the use of a frequency dependent complex density matrix. The main parameter ruling the viscous losses is the permeability (or the flow resistivity). This is a macroscopic measurable parameter. The viscous frictions can be considered to represent a third type of coupling in porous media, in addition to inertial and elastic coupling. For air-saturated materials, Champoux and Allard [8] and Lafarge et al. [9] have shown that thermal exchanges are non negligible and must be included as an additional loss mechanism.

Biot has shown the existence of two frequency regimes separated by a characteristic frequency given by

$$f_c = \frac{\eta\phi^2}{k_0} \tag{1}$$

where ϕ the porosity and k_0 the static permeability. The relevant model parameters and the context in which they were introduced are described in more details in the next sections. The fast wave is propagative in the all

frequency range but is dispersive due to the couplings and the attenuation mechanisms. In the low frequency regime (below f_c), the slow wave is diffusive, does not propagate and the fluid and solid displacements are in phase opposition. Above the characteristic frequency, the slow wave is propagative.

It is important to notice that Biot's theory describes Poiseuille viscous flows along the pores and is relevant when the viscous skin depth is of the order or smaller than the characteristic size of the pores. The viscous skin depth is given by $\delta = (2\eta/\omega\rho_f)^{1/2}$ where η is the fluid dynamic viscosity, ρ_f the density of the fluid and ω the angular frequency. As an example, a material containing pores of a few dozens nanometer such as those used in filtration in chemistry has a very low the permeability k_0 is very low. Usual acoustic measurements will be located very low in Biot's low frequency range and the materials will behaves like non-porous homogeneous material. The Biot model is valid for these materials but probably without much interest for relatively viscous fluids.

At higher frequencies, the viscous skin depth becomes smaller than the pore size. The complexity of the pore shape cannot be accounted for by the static permeability alone and the high frequency parameters of Attenborough [10, 11], Johnson et al. [12] and of Allard [3] play an important role.

2.2 Wave propagation in the rigid frame approximation

In many situations for air-filled materials, the porous frame can be considered to be much more rigid and heavier than air and a simplified model can be used. The main physical parameters can be introduced in this approximation. The mechanical properties of the solid skeleton will be investigated later in this study.

In the rigid frame approximation, the solid is incompressible and does not move and only the fluid-borne wave can propagate. Its complex density and compressibility are given by

$$\rho(\omega) = \alpha_\infty \rho_f \left(1 - j\frac{\omega_c}{\omega} F(\omega)\right) \tag{2}$$

$$K(\omega) = \frac{\gamma P_0}{\gamma - (\gamma - 1)\left(1 - j\frac{\omega_c}{B^2\omega} G(B^2\omega)\right)^{-1}} \tag{3}$$

where α_∞ the tortuosity, B^2 the Prandtl number and γ the specific heat ratio of the fluid at constant pressure and volume. $F(\omega)$ and $G(B^2\omega)$ are respectively viscosity and thermal correction functions for high frequencies including the high frequency parameters.

The complex density is related to the existence of inertia and viscous forces while the complex bulk modulus includes thermal exchanges between the solid and the fluid. All the necessary properties e.g. the propagation constant, the phase velocity and the attenuation of the fluid borne wave can be deduced from the complex density and bulk modulus.

2.3 Other models and parameters

The full Biot model is accepted as one of the most general model for the description of propagation porous solid with elastic frame and most of the models developed after Biot are only concerned with the evaluation of the functions $F(\omega)$ and $G(B^2\omega)$. This section gives a brief review of these models and of the parameters introduced. These parameters were defined in the rigid frame approximation.

The first parameter of importance with the phase densities is the porosity. The open porosity is the ratio of the volume of the pores connected together and to the exterior and the total volume of the sample:

$$\phi = V_{Pores}/V_{Total} \tag{4}$$

A closed porosity corresponding to inclusions in the solid is also defined.

In addition to the porosity and the densities, the flow resistivity or the flow permeability have rapidly been identified as parameters of importance for the acoustic modeling, resulting in simple semi-empirical models [15]-[18]. The flow resistivity σ is defined as the coefficient relating the pressure gradient $\frac{\Delta P}{l}$ across a distance (thickness) l to the resulting volume flow of fluid per unit area Q.

$$\Delta P/l = \sigma Q \tag{5}$$

The flow resistivity of polyurethane foams used in acoustics varies typically between 10^3 Ns/m^4 and 10^5 Ns/m^4. The (static) permeability is often used instead of the flow resistivity, in particular by geophysicists. In acoustics, the static flow can be considered to be the low frequency limit of the dynamic flow associated with the wave propagation. The dynamic flow corresponds to a fluid moving to and fro in the pores. The permeability is defined as

$$k_0 = \eta/\sigma \tag{6}$$

This is a material constant and is independent of the saturating fluid.

In the framework of Biot's theory, important contributions were offered by Attenborough, Johnson et al. and Allard. Attenborough [10, 11] showed the importance of *tortuosity* and of parameters related to the complexity of the pore geometry at high frequencies. The tortuosity characterizes the sinuous aspect of the fluid flow associated with the passage of a wave in a porous medium. The tortuosity and the two characteristic lengths presented next are defined in Biot's high frequency limit (see Figure 2) when the viscous skin depth is small compared to the pore size. It is therefore defined for a inviscid fluid as

$$\alpha_\infty = \frac{\frac{1}{V}\int_V v^2 dV}{\left(\frac{1}{V}\int_V \vec{v} dV\right)^2} \tag{7}$$

where the integration is carried out over a volume V greater than the minimum volume of homogenization. v is the microscopic flow velocity in the pores and $\vec{v}$ is the velocity along the propagation vector. The tortuosity can also be defined from the ratio of the path in the pores between two points on the propagation axis in the porous medium separated by a great distance and the length of the straight line joining the points. The tortuosity is always greater than 1. For cylindrical pores with a constant diameter and at an angle θ with the propagation vector (Figure 3), $\alpha_\infty = 1/cos^2\theta$. Brown [13] has shown that the tortuosity can be evaluated from the measurement of the electrical conductivity. The method has been optimized by Champoux [14].

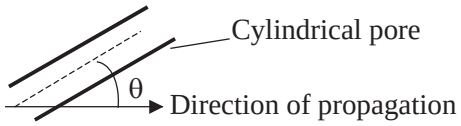

Figure 3: Cylindrical pore at an angle θ with the wave vector.

Johnson et al. [12] contributed substantially by introducing the concepts of *dynamic tortuosity and permeability* for the description of viscous interaction between the solid and the fluid at high frequencies. Johnson et al. also introduced the concepts of viscous characteristic length Λ in order to integrate the complexity of the pore shape at high frequencies during viscous flows. The viscous characteristic length Λ is defined as

$$\frac{2}{\Lambda} = \frac{\int_A v^2(r_w) dA}{\int_V v^2(r) dV} \tag{8}$$

where $v(r)$ and $v(r_w)$ are respectively the microscopic fluid velocities in the pore volume and on the pore walls. Λ was introduced to account for viscous frictions between the solid and the fluid. For air-filled materials, Champoux and Allard [8] defined a thermal characteristic length Λ', Lafarge et al. [9] defined a dynamic compressibility of the fluid including this length. The thermal characteristic length Λ' is given by

$$\frac{2}{\Lambda'} = \frac{\int_A dA}{\int_V dV} \tag{9}$$

which is similar to the viscous characteristic length with the difference that the weight v^2 in the integrals have disappeared. The thermal characteristic length therefore represents the average ratio of the pore volume to their surface. Figure 4 shows an example of pore. The definitions of Λ and of Λ' are such that the regions of constriction (region 1 on Figure 4) have a great influence on the viscous length while open regions (region 2 on Figure 4) mainly contribute to the thermal characteristic length. Indeed, the flow velocities are greater at the constrictions and contribute more to the integrals (8) than more open regions. On the other hand, the average pore volume-to-surface ratio is mainly determined by open regions where the exchange area between the solid and the fluid is greater.

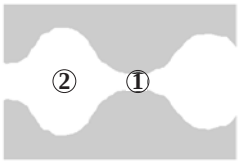

Figure 4: Example of pore. Region 1: constriction, region 2: open region.

The more recent refinements include the concepts of thermal permeability [19] related to the trapping constants [20] and a modification of the model of Johnson et al. providing a new low frequency limit for the dynamic permeability [21].

Umnova et al. [22] have proposed a model of the propagation in granular media based on the existence of a cell of influence around the particles.

Burridge and Keller [23] have shown that Biot's equations of poroelasticity could be obtained under certain conditions on the viscosity from a homogenization method. Auriault et al. [24] have also applied a homogenization method to a periodic deformable medium to obtain results similar to Biot's and a generalization of Darcy's law providing generalized permeability coefficients. The homogenization theory is beyond our domain of investigation and only the physical parameters of Biot's theory and of the models derived from this theory are studied.

3 Impedances and acoustical properties of porous layers

The acoustical properties of porous layer e.g. their surface impedance, reflection coefficients, absorption coefficients can be deduced from the complex density and the compressibility (Equation 3 and 4). From these, the complex wave velocity is given by

$$V_\varphi = \sqrt{K(\omega)/\rho(\omega)} \tag{10}$$

The characteristic impedance is defined for an infinite porous medium as the ratio of the pressure and the of particle velocity. In the rigid frame approximation, it is given by

$$Z_C = \rho(\omega)V_\varphi(\omega) = \sqrt{\rho(\omega)K(\omega)} \tag{11}$$

Consider at the interface between a fluid and a porous medium two points M_1 and M_2 infinitely close from one another, one being in the fluid and the other in the porous medium. From references [25, 3], it can be shown that the relationship between the impedances at M_1 and M_2 is

$$Z(M_2) = Z(M_1)/\phi \tag{12}$$

This relationship is very useful for calculating the surface impedance of finite thickness materials mounted in certain conditions. As an example, the surface impedance of a porous layer of thickness d applied on a rigid substrate is given by

$$Z(M_2) = -jZ_C cot\left(k(\omega)d\right)/\phi \tag{13}$$

where the complex wavenumber is given by

$$k(\omega) = \omega/V_\varphi \tag{14}$$

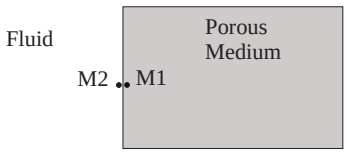

Figure 5: Interface between a fluid and a porous medium.

Following, the same method, it is possible to calculate the transmission and reflection coefficients of a porous layer surrounded by air. It can also be shown that the pressure and particle velocity on one side of the porous layer can be expressed as a function of the pressure and velocity on the opposite side through a transfer matrix [26, 3]. This elegant formulation yields the acoustical properties of multilayer porous systems.

4 Evaluation of high frequency parameters by ultrasonic measurements

4.1 The method of Allard et al. [27] for measuring the tortuosity

The phase velocity and attenuation of the wave can be calculated from the expression of the complex wave velocity and plotted versus frequency as shown in the example of Figure 6.

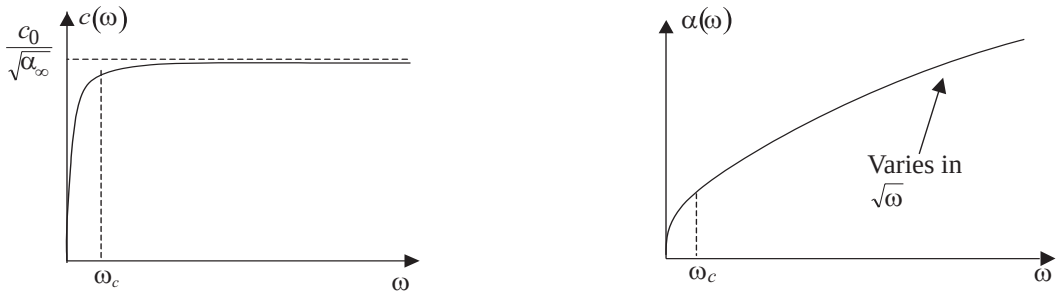

Figure 6: Phase velocity and attenuation of the fluid borne wave in a rigid frame porous medium. c_0 is the sound speed in air

The wave is highly dispersive at low frequencies (below $\omega_c = 2\pi f_c$) and its phase velocity tends at high frequencies to a limit that is lower than the free velocity in air. The attenuation increases with frequency. However, the rate of increase of attenuation is higher at low frequencies, which means that the attenuation per cycle is greater at low frequencies. In the high frequency limit, it can be shown that the attenuation varies as the square root of frequency. At sufficiently high frequencies i.e. when the viscous skin depth is sufficiently smaller than the pore size, the wavenumber tends to

$$k(\omega) = \omega \frac{\sqrt{\alpha_\infty}}{c_0} \left[1 + \frac{\delta(1-j)}{2} \left(\frac{1}{\Lambda} + \frac{\gamma - 1}{\Lambda' B} \right) \right] \tag{15}$$

The high frequency limit of the phase velocity has been used by Allard et al. [27] for determining the tortuosity. Their experimental principle is simple. It consists in deducing information in the frequency domain from the signal transmitted in an air saturated porous layer in the high frequency limit. The ultrasonic emitter and receiver used are air coupled capacitive transducer with vibrating mylar membranes. The ultrasonic frequency range investigated depends on the thickness of the mylar membranes. Figure 7 shows an example of reference signal (without sample between the transducers) and transmitted signal.

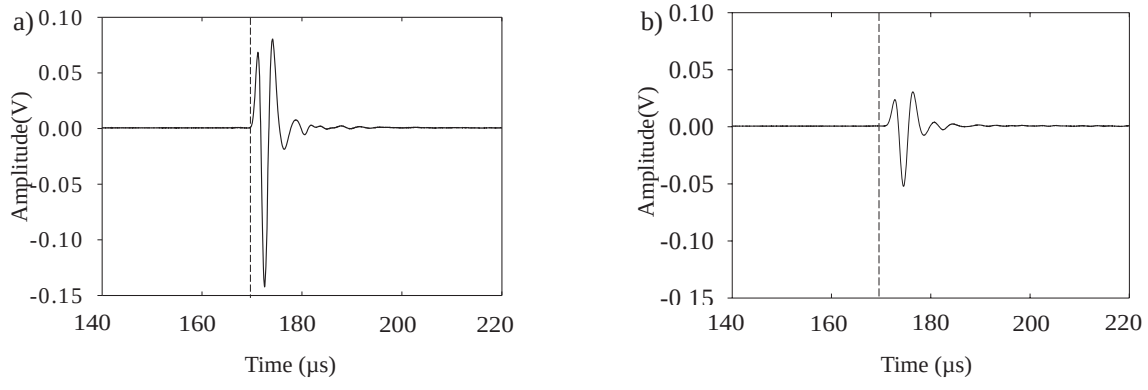

Figure 7: Signal received by the ultrasonic receiver a) without sample between the emitter and receiver, b) after transmission through a porous layer

The method of Sachse and Pao [28] is used for the determination of the phase velocity from experimental results. The phase velocity is obtained from the phase difference between the signal obtained without sample between the transducers (reference signal) and the signal received when the wave has crossed the sample. The attenuation is deduced from the magnitudes of the spectra of the reference and received signals.

The method of Allard et al. [27] for measuring the tortuosity consists in determining the high frequency limit of the phase velocity in Figure 8. When the viscous skin depth tends to zero in equation 16, this limit velocity is $c_0/\sqrt{\alpha_\infty}$

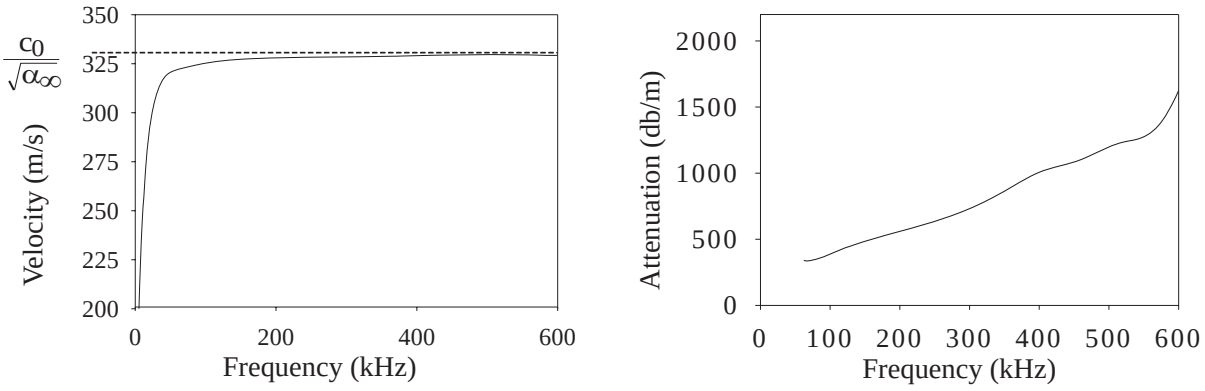

Figure 8: Phase velocity and attenuation in a polyurethane foam

4.2 Methods for measuring α_∞, Λ and Λ'

These methods are inspired from the works by Johnson et al. [12, 29, 30] on the wave propagation in porous media saturated by super fluid He, of Nagy [31] and of Allard et al. [27] on the propagation in air-saturated materials at ultrasonic frequencies.

4.2.1 The $Q\delta$ method

The $Q\delta$ method is based on the behavior of the quality factor Q in the high frequency limit. The quality factor is a function of the real and imaginary parts of the complex wavenumber $Q = k'/2k''$. From the expression 16 for the wavenumber, it can be seen that the product $Q\delta$ tends to [32]

$$\lim_{\omega\to\infty} Q\delta \;=\; \left[\frac{1}{\Lambda} \;+\; \frac{\gamma \;-\; 1}{B\;\Lambda'}\right]^{-1} \tag{16}$$

and depends only on known gas constants (γ, B) and on the lengths Λ and Λ'. This limit value (the length $[1/\Lambda + (\gamma-1)/(B\Lambda')]^{-1}$) is shown by the arrow in Figure 9a.

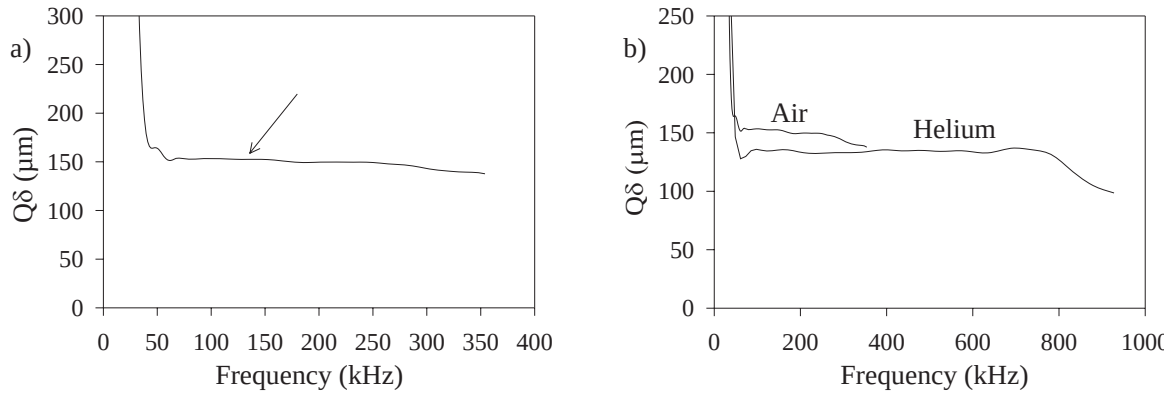

Figure 9: a) High frequency limit of the $Q\delta$ product. b) $Q\delta$ product measured in a porous material saturated successively by two different gases

Now, if the ultrasonic experiments are carried out in porous materials saturated successively by different gases, say air and then helium, the following system is obtained [33]:

$$\lim_{\omega\to\infty} (Q\delta)_{air} \;=\; \left[\frac{1}{\Lambda} \;+\; \frac{\gamma_{air} \;-\; 1}{B_{air}\;\Lambda'}\right]^{-1} \tag{17}$$

$$\lim_{\omega\to\infty} (Q\delta)_{he} \;=\; \left[\frac{1}{\Lambda} \;+\; \frac{\gamma_{he} \;-\; 1}{B_{he}\;\Lambda'}\right]^{-1} \tag{18}$$

providing two different limits for the $Q\delta$ product as shown in Figure 9b. Reading the two limit values and solving the system above yields values of Λ and Λ' with the same precision.

4.2.2 The n^2 method

This method is based on the refraction index n i.e. the ratio of the reference velocity in the free gas and the velocity in the porous medium. It can be shown that at high frequencies [33]:

$$n^2 = \alpha_\infty \left[1 + \delta \left(\frac{1}{\Lambda} + \frac{\gamma - 1}{\Lambda' B}\right)\right] \tag{19}$$

since the viscous skin depth varies as the inverse of the square root of frequency, plotting n^2 as a function of $f^{-1/2}$ provides a straight line with a slope proportional to the quantity $[1/\Lambda + (\gamma - 1)/(B\Lambda')]$ while the intercept with the vertical axis yields the tortuosity [34]. Here again, the experiments in two saturating gases yield the two unknowns Λ and Λ' with the same precision [33]. Figure 10 shows an example of experimental result, with the determination of α_∞, Λ and Λ'

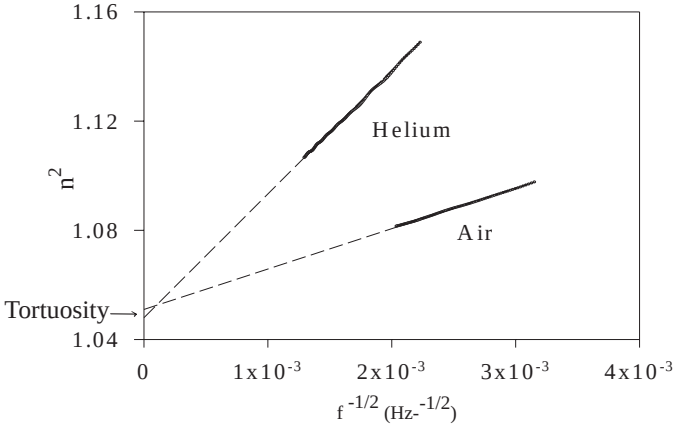

Figure 10: n^2 as a function of $f^{-1/2}$ in helium and in air

Table 1 summarizes results obtained from different methods for three different polyurethane foams. The last column of the table corresponds to BET measurements made in Laboratoire de Chimie des Surfaces de l'université Pierre et Marie Curie. The BET method is named after Brunauer, Emmet and Teller [35, 36]. The $Q\delta$ and the n^2 methods show a good consistency for the values of Λ and of Λ' while the BET method seems to slightly overestimate the value of Λ'.

	$\Lambda(Q\delta)$	$\Lambda(n^2)$	$\Lambda'(Q\delta)$	$\Lambda'(n^2)$	$\Lambda'(BET)$
Foam 1	180	202	429	367	610
Foam 2	132	134	292	318	370
Foam 3	249	273	650	672	750

Table 1: Results on different foams (all values are in μm).

4.2.3 Measurement of ϕ and α_∞ from ultrasonic reflection and time domain analysis of the signal

Fellah and Depollier [40] have proposed a time domain approach of the transient wave propagation in porous media including the description of the transient behavior. Following this work and the ultrasonic methods cited above, new methods were developed [38, 39], based on the reflection or transmission of ultrasonic waves. Low permeability materials such as non reticulated materials have generally a higher reflection coefficient than materials with open cells and working in reflection results in a higher signal to noise ratio for these materials.

A particularly interesting application is the measurement of the porosity and or the tortuosity from ultrasonic wave reflected at high frequencies at the interface between a highly resistive porous material and air. Fellah at al [39] have established an expression of the normal incidence reflection coefficient in the high frequency limit

$$R = \frac{\frac{\alpha_\infty cos\theta}{\phi\sqrt{\alpha_\infty - sin^2\theta}} - 1}{\frac{\alpha_\infty cos\theta}{\phi\sqrt{\alpha_\infty - sin^2\theta}} + 1} \tag{20}$$

where θ is the angle of incidence. This expression can be used to determine the tortuosity if the porosity is known for example. The time signals of the incident and reflected waves are similar in shape to those of Figure 7.

4.3 Ultrasonic scattering and high frequency limit of the classical models

Figure 9b shows that the product $Q\delta$ drops from a frequency around 250 kHz for the experiment in air and 760 kHz in helium. This behavior is a consequence of an extra attenuation, not predicted by Biot's theory or other classical models and occurring at higher frequencies. The consequence is a decrease of the quality factor (the inverse of the attenuation per cycle) and of the product $Q\delta$. This additional attenuation was first observed in natural and artificial air-saturated porous sandstones by Nagy [31].

Leclaire et al. [37] have shown that only scattering is responsible for the extra attenuation observed in highly porous polyurethane foams and have proposed a scattering model where a collection of identical rigid cylinders (Neuman cylinders) are considered as scatterers. The model only considers simple scattering and is valid for a low concentration of scatterers and in the low frequency domain of the scattering models. A fairly good theoretical/experimental match was obtained as the assumptions made apply fairly well to materials studied.

Although extremely interesting for the physical description of the wave propagation in porous media at frequencies above Biot's high frequency regime, scattering is an undesired phenomenon in the measurement of the high frequency parameters.

5 Elastic and viscoelastic properties of porous materials

The elastic properties of the solid frame play a role in the full Biot model, with elastic frame. In order to complete the characterization of porous acoustic materials, new techniques for evaluating the elastic and viscoelastic properties are presented.

5.1 Classical methods

Classical methods for measuring the elastic coefficients of porous materials exist. These are based on a transfer function $H(\omega)$ between the source and the detector and involve the excitation of a sample of a certain shape (e.g. a rod, a cube, a plate...). The sample has a finite size with respect to the wavelengths involved i.e. its dimensions are smaller or of the order of the wavelengths studied. Examples are reported by T. Pritz and other authors [41, 42, 43]. Figure 11 shows possible devices for the measurement of Young's modulus and of the Poisson ratio. The properties (resonance frequencies, damping, dynamic behavior) of the complex transfer function between the response and the excitation yield the mechanical properties of the structure excited. However, the frequency described in these methods are fairly low (typically below 500 Hz for some materials).

5.1.1 The transfer function method

In Figure 11a, a shaker (shaker 1) fed with a white noise signal excites with compressional waves a sample with the shape of a rod. Neglecting the effect of the air in the pores, the Young's modulus of the porous frame is then evaluated from the transfer function $H(\omega)$ between the two accelerometer glued at the extremities of the rod, one accelerometer being attached to the source. A second shaker can also be used (independently from the first shaker) to generate torsions in the sample, providing information on the shear modulus and on the Poisson ratio. In this case, a second pair of accelerometers oriented differently are used.

Figure 11b shows a setup used for evaluating the shear modulus. Two identical pieces of sample are glued to a rigid metal frame and to a thin, movable plate connected to a shaker. The shaker generates shear waves in the sample and an impedance head measures the force applied. The transfer function between the force F applied and the acceleration a at the output of the impedance head shows the resonance frequencies in the sample. From the resonance frequencies of the transfer function, the density and the thickness of the sample, the magnitude of the shear modulus can be determined. From the width at half height of the resonance peaks, the loss angle can be determined. By performing the experiment with samples with different thicknesses, information about the frequency dependence of the shear modulus can be obtained. Figure 12 shows a typical transfer function for the measurement of shear modulus. Up to three resonance frequencies can be observed, decreasing in amplitude due to the damping in the sample.

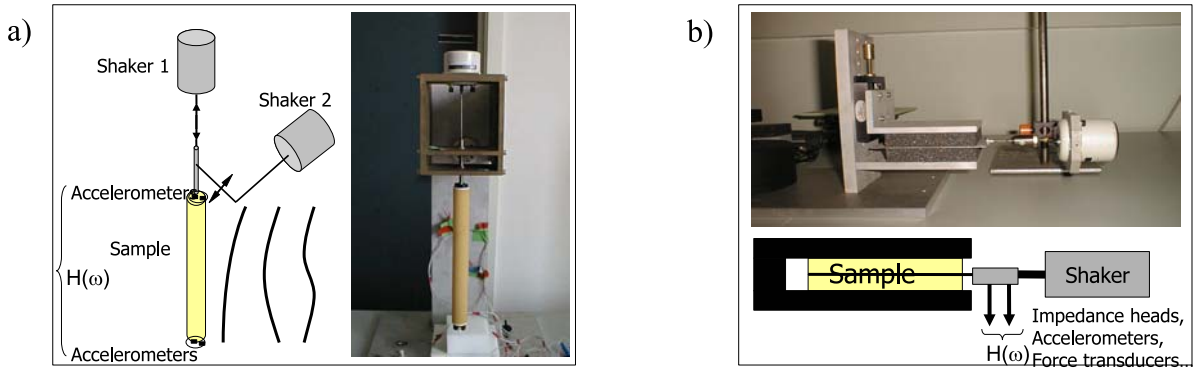

Figure 11: Possible setups for the measurement of a) Young's modulus, b) shear modulus.

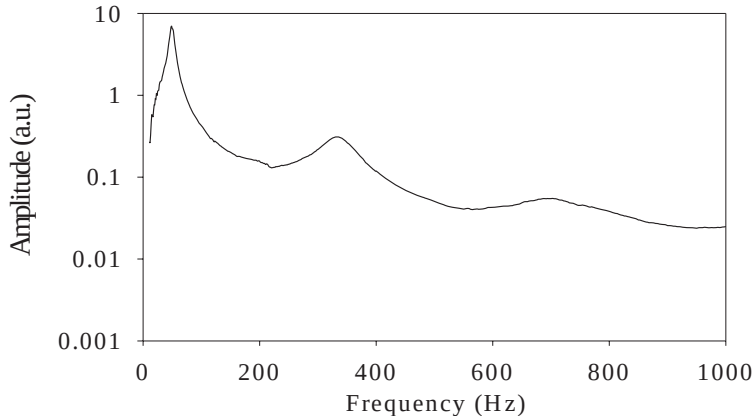

Figure 12: Shape of the transfer function between force and acceleration in the experiment of Figure 11b.

5.1.2 The Oberst beam method

This method consists in setting the sample in the configuration of a multilayer cantilever beam including the base beam (e.g. aluminum or steel beam), the unknown material on top of the base beam and optionally, a third layer of another material. The rest of the method follows the transfer function method. An analytical or numerical model can be used to describe the vibration of the multilayer system and to relate it to the elastic properties of the unknown material. More details and variants of this method in one or two dimensions were recently given by Jaouen [44]. The method has been applied to a highly porous Melamine foam.

5.1.3 The temperature - frequency equivalence

It has been observed that the behavior of a viscoelastic material at high temperature for low frequencies is equivalent to the behavior of the same material at lower temperature and for proportionally higher frequencies. This equivalence is illustrated in Figure 13 and can be exploited to overcome the problem of high damping at higher frequencies in the experiment. However in this method, the data points are not truly 'measured'.

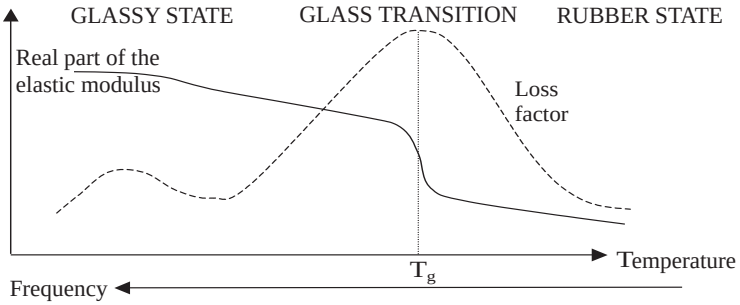

Figure 13: Real part of the elastic modulus and loss factor of a polyurethane foam during the glass transition.

5.2 The Rayleigh wave method

Allard et al. [45] have studied the Rayleigh structure borne surface wave in soft porous materials, with the determination of the shear modulus at very high frequencies as a direct application.

A shaker excites the surface of a large thick block of foam with a narrow-band sine burst at a high frequency. The vertical velocity component of the surface is measured at incrementing distances from the source with the help of a Polytec vibrometer. The surface wave is non dispersive and the signal is simply delayed (and attenuated) as the detector moves away fro the source. The calculation of the cross-correlation between the signal at different position provides the phase velocity. Results have been obtained in a frequency range typically between 3 and 4 kHz on a block of highly porous polyurethane foam.

5.3 The guided wave method

Extending the work of Allard et al., Boeckx et al. [46, 47] have recently presented results on the propagation of guided waves in layers of poroelastic materials. These experiments, together with a complete theoretical description have provided information on the complex shear modulus in a frequency range that covers both the low frequencies of the classical methods and the high frequency limit of the Rayleigh wave method. A new experimental method was proposed for the determination of the dispersion curves of guided waves in poroelastic layers. This method is based on the excitation and detection of standing wave and on the spatial Fourier transformation of the standing wave profile of the surface.

The standing waves are generated by line source attached to a shaker producing a continuous sinusoidal wave with frequencies that can be varied. The particle velocity of the surface of the layer is measured with a laser Doppler vibrometer. The laser beam at the output of the laser is collimated and a mirror/lens arrangement insures that the beam is always focused on the surface at any position of the beam. The measurement point can be moved by moving the mirror/lens arrangement. A strip of reflective tape is used to reflect the laser beam in the path of the scanning beam. For each frequency, the path is scanned with a typical step of 1 to 5 mm and the amplitude and phase of the signal are recorded at each position.

Once the data are recorded, the spatial Fourier Transform of the displacement profile in the vicinity of the rigid end can be calculated. The different amplitude peaks in the spatial spectrum provide the wavenumbers of all the guided modes propagating in the layer and the phase velocities are obtained from dividing the frequency by these wavenumbers.

The use of guided waves and an excitation by continuous sine wave present the advantages of concentrating the energy in a layer of material and at a single frequency. This results in the possibility to increase the propagation distance and in maximizing the signal to noise ratio.

Two experimental configurations were proposed: a layer of porous material glued on a rigid substrate and a porous layer under Lamb conditions (Figure 14). Figure 15 shows the calculated dispersion curves for the porous layer under Lamb conditions. The experimental dispersion curves obtained from the measurement described above are shown in Figure 16 and compared to the theoretical results for 2 different materials.

The fitting of at least two theoretical dispersion curves to the experimental data allows to investigate both the real and imaginary parts shear in the frequency range between the classical vibration method and the Rayleigh wave propagation method (Figure 17). In addition to the frequencies, the exploitation of the amplitudes of the different modes in the wavenumber space (spatial Fourier Transform of the standing wave pattern) should provide more information and allow the study of both the real and imaginary parts of the shear modulus and of Young's modulus.

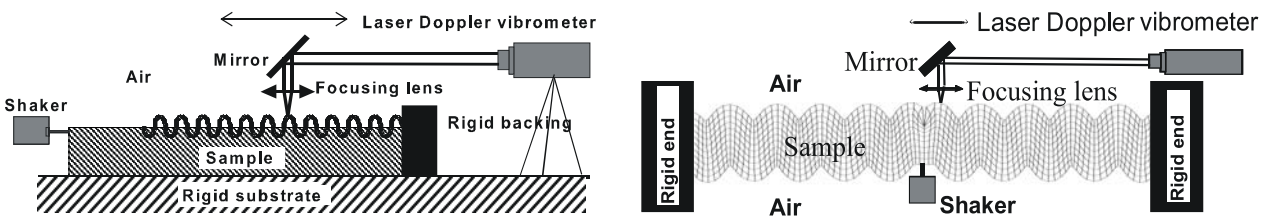

Figure 14: Experimental configurations for the study of guided waves in porous layers.

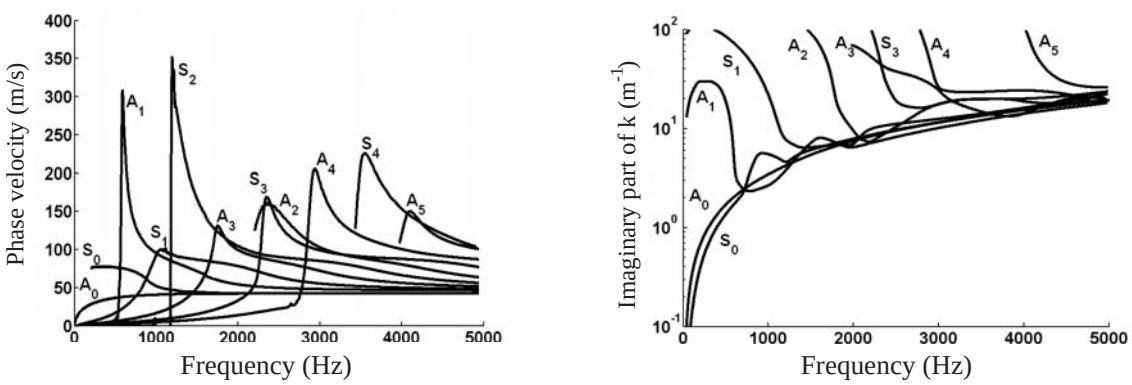

Figure 15: Theoretical dispersion curves for a layer of porous material saturated by air under Lamb conditions.

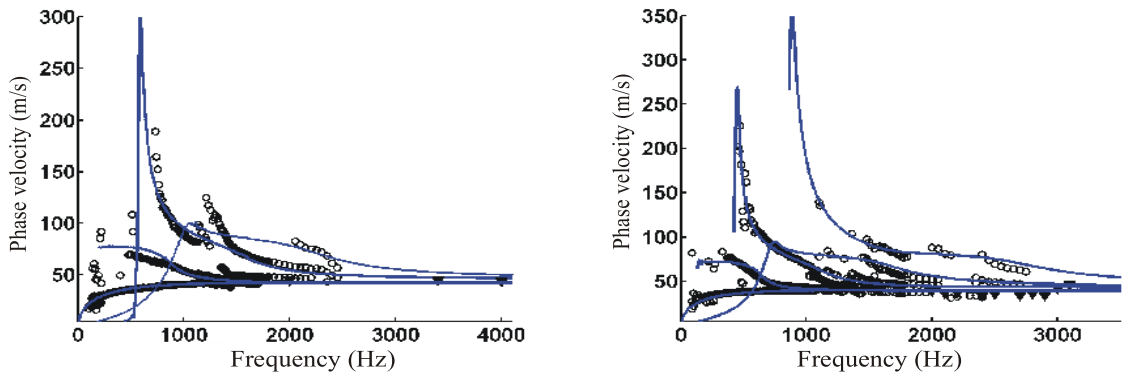

Figure 16: Experimental results on the dispersion curves.

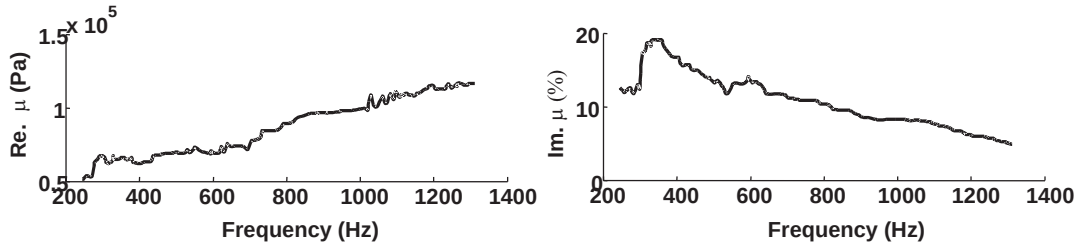

Figure 17: Fitted real and imaginary parts of the shear modulus of a highly porous foam (Melamine). The configuration used is that of a layer on a rigid substrate.

References

[1] O. C. Zwikker and C. W. Kosten, *Sound-Absorbing Materials*, Elsevier, 1949.

[2] M. A. Biot, *Theory of elastic wave propagation in a fluid saturated porous solid*, J. Acoust. Soc. Am. **28**, pp. 168-191, 1956.

[3] J. F. Allard, *Propagation of Sound in Porous Media: Modeling Sound Absorbing Materials*, Chapman & Hall, London, 1993.

[4] L. L. Beranek, *Acoustic impedance of porous materials*, J. Acoust. Soc. Am. **13**, pp. 248-260, 1942.

[5] Y. Champoux, M. R. Stinson and G. A. Daigle, *Air-based system for the measurement of porosity*, J. Acoust. Soc. Am. **89**, pp. 910-916, 1991.

[6] ISO 9053: *Acoustics - Materials for acoustical applications - Determination of airflow resistance*, 1991.

[7] M. A. Biot and D. G. Willis, *The elastic coefficients of the theory of consolidation*, J. Appl. Mech. **24**, pp. 594-601, 1957.

[8] Y. Champoux and J. F. Allard, *Dynamic tortuosity and bulk modulus in air saturated porous media*, J. Appl. Phys. **70**, pp. 1975-1979, 1991.

[9] D. Lafarge, P. Lemarinier, J. F. Allard and V. Tarnow, *Dynamic compressibility of air in porous structures at audible frequencies*, J. Acoust. Soc. Am. **102**, pp. 1995-2006, 1997.

[10] K. Attenborough, *Acoustical characteristics of porous materials*, Physics reports **82**, pp. 179-227, 1982.

[11] K. Attenborough, *Acoustical characteristics of rigid fibrous absorbents and granular materials*, J. Acoust. Soc. Am. **73**, pp. 785-799, 1983.

[12] D. L. Johnson, J. Koplik and R. Dashen, *Theory of dynamic permeability and tortuosity in fluid-saturated porous media*, J. Fluid. Mech. **176**, pp. 379-402, 1987.

[13] R. Brown, *Connection between the formation factor for electrical resistivity and fluid-solid coupling factors in Biot's equations for acoustic waves in fluid-filled porous media*, Geophysics **45**, pp. 1269-1275, 1980.

[14] Y. Champoux, *Etude expérimentale du comportement acoustique des matériaux poreux à structure rigide*, PhD thesis, Carlton University, Canada, 1991.

[15] M. E. Delany and E. N. Bazley, *Acoustical characteristics of fibrous absorbent materials*, Appl. Acoust. **3**, pp. 105-116, 1970.

[16] Y. Miki, *Acoustical models of porous materials - Modification of Delany-Bazley model*, J. Acoust. Soc. of Japan **11**, pp. 19-24, 1990.

[17] D. K. Wilson, *Relaxation-matched modeling of sound propagation in porous media, including fractal pore surfaces*, J. Acoust. Soc. Am. **94**, pp. 1136-1145, 1993.

[18] N. Voronina, *Acoustic properties of fibrous materials*, Appl. Acoust. **42**, pp. 65-174, 1994.

[19] D. Lafarge, *Propagation du son dans les matériaux poreux à structure rigide saturés par un fluide viscothermique: définition des paramètres géométriques, analogie électromagnétique, temps de relaxation*, PhD thesis Université du Maine, France, 1993.

[20] A. Debray, J. F. Allard, W. Lauriks and L. Kelders, *Acoustical measurement of the trapping constant of porous materials*, Rev. Sci. Inst. **68**, pp. 4462-4464, 1997.

[21] S. R. Pride, F. D. Morgan and A. F. Gangi, *Drag force of porous medium acoustics*, Phys. Rev. B **47**, pp. 4964-4978, 1993.

[22] O. Umnova, K. Attenborough and K. M. Li, *A cell model for the acoustical properties of packings of spheres*, Acustica-Acta Acustica **87**, pp. 226-235, 2001.

[23] R. Burridge and J. B. Keller, *Poroelasticity equations derived from microstructure*, J. Acout. Soc. Am. **70**, pp. 1140-1146, 1981.

[24] J. L. Auriault, L. Borne and R. Chambon *Dynamics of porous saturated media, checking the generalized law of Darcy*, J. Acout. Soc. Am. **77**, pp. 1641-1650, 1985.

[25] H. Deresiewicz and R. Skalak, *On uniqueness in dynamic poroelasticity*, Bull. Seism. Soc. Am. **53**, pp. 783-788, 1963.

[26] W. Lauriks, P. Mees and J. F. Allard, *The acoustic transmission through layered systems*, J. Sound Vib. **155**, pp. 125-132, 1992.

[27] J. F. Allard, B. Castagnède, M. Henry and W. Lauriks, *Evaluation of the tortuosity in acoustic porous materials saturated by air*, Rev. Sci. Inst. **65**, pp. 7654-755, 1994.

[28] W. Sachse and Y. Pao, *On the determination of phase and group velocities of dispersive waves in solids*, J. Appl. Phys. **49**, pp. 4320-4327, 1980.

[29] D. L. Johnson, T. J. Plona, C. Scala, F. Pasierb and H. Kojima, *Tortuosity and acoustic slow waves*, Phys.Rev.Lett. **49**, pp. 1840-1844, 1982.

[30] D. Singer, F. Pasierb, R. Ruel and H. Kojima, *Multiple scattering of second sound in superfluid II-filled porous medium*, Phys. Rev. B **30**, pp. 2909-2912, 1984.

[31] P. B. Nagy, *Slow wave propagation in air-filled permeable solids*, J. Acoust. Soc. Am. **93**, pp. 3224-3234, 1993.

[32] P. Leclaire, L. Kelders, W. Lauriks, C. Glorieux and J. Thoen, *Determination of the viscous characteristic length in air-filled porous materials by ultrasonic attenuation measurements*, J. Acoust. Soc. Am. **99**, pp. 1944-1948, 1996.

[33] P. Leclaire, L. Kelders, W. Lauriks, M. Melon, N. Brown, and B. Castagnède, *Determination of the viscous and thermal characteristic lengths of plastic foams by ultrasonic measurements in helium and air*, J. Appl. Phys. **80**, pp. 2009-2012, 1996.

[34] N. Brown, M. Melon, V. Montembault, B. Castagnède, W. Lauriks and P. Leclaire, *Evaluation of the viscous characteristic length of air saturated porous materials from the ultrasonic dispersion curve*, C. R. Acad. Sci. Paris **322 Série IIb**, pp. 121-127, 1996.

[35] S. Brunauer, P. H. Emmet and E. Teller, *Adsorption of gases in multimolecular layers*, J. Am. Chem. Soc. **60**, pp. 309-319, 1938.

[36] P. Lemarinier, M. Henry, J. F. Allard, J. L. Bonardet and A. Gdon, *Connection between the dynamic bulk modulus of air in a porous medium and the specific surface*, J. Acoust. Soc. Am. **97**, pp. 3478-3482, 1995.

[37] P. Leclaire, L. Kelders, W. Lauriks, J. F. Allard and C. Glorieux, *Ultrasonic wave propagation in reticulated foams saturated by different gases - High frequency limit of the classical models*, Appl. Phys. Lett. **69**, pp. 2641-2643, 1996.

[38] Z. E. A. Fellah, C. Depollier, S. Berger, W. Lauriks, P. Trompette and J. Y. Chapelon, *Determination of transport parameters in air-saturated porous materials via reflected ultrasonic waves*, J. Acoust. Soc. Am. **114**, pp. 2561-2569, 2003.

[39] Z. E. A. Fellah, S. Berger, W. Lauriks, C. Depollier, C. Aristegui and J. Y. Chapelon, *Measuring the porosity and the tortuosity of porous materials via reflected waves at oblique incidence*, J. Acoust. Soc. Am. **113**, pp. 2424-2433, 2004.

[40] Z. E. A. Fellah and C. Depollier, *Transient acoustic wave propagation in rigid porous media: A time-domain approach*, J. Acoust. Soc. Am. **107**, pp. 683-688, 2000.

[41] T. Pritz, *Transfer function method for investigating the complex modulus of acoustic materials: rod-like specimen*, J. Sound Vib. **81**, pp. 359-376, 1982.

[42] A. Sfaoui, *On the viscoelasticity of the polyurethane foam*, J. Acoust. Soc. am. **97**, pp. 1046-1052, 1995.

[43] T. Pritz, *Dynamic Young's Modulus and loss factor of plastic foams for impact sound isolation*, J. Sound Vib. **178**, pp. 315-322, 1994.

[44] L. Jaouen, *Contribution à la caractérisation mécanique de matériaux poro-viscoélastiques en vibroacoustique*, PhD thesis Université du Maine, France, et Université de Sherbrooke, Canada, 2003.

[45] J. F. Allard, G. Jansens, G. Vermeir and W. Lauriks, *Frame-borne surface waves in air-saturated porous media*, J. Acoust. Soc. am. **111**, pp. 690-696, 2002.

[46] L. Boeckx, P. Leclaire, P. Khurana, C. Glorieux, W. Lauriks and J. F. Allard, *Investigation of the phase velocities of guided acoustics waves in soft porous layers*, J. Acoust. Soc. Am. **117**, pp. 545-554, 2005.

[47] L. Boeckx, P. Leclaire, P. Khurana, C. Glorieux, W. Lauriks and J. F. Allard, *Guided elastic waves in porous materials saturated by air under Lamb conditions*, J. Appl. Phys. **97**, pp. 094911-8, 2005.